

# Field Programmable Analog Array (FPAA) based Control of an Atomic Force Microscope

Georg Schitter\*

Delft Center for Systems and Control  
Delft University of Technology  
Mekelweg 2, 8c-3-22  
2628 CD Delft, The Netherlands

Nghi Phan

Veeco Metrology Inc.  
112 Robin Hill Rd.  
Santa Barbara, CA-93117  
USA

**Abstract**—For topography measurements and faster imaging with the AFM a high control-bandwidth is required. This paper presents an analog implementation of a model-based controller for a high-speed Atomic Force Microscope (AFM) using a new type of control hardware. The vertical positioning axis of the AFM scanner is modeled, and the imaging bandwidth is improved by means of model-based control. The new feedback controller, which is designed in the  $H_\infty$ -framework, is implemented on a Field Programmable Analog Array (FPAA), which enables operation of the model-based controlled AFM system at a feedback bandwidth on the order of 100 kHz. Measured results demonstrate that the closed-loop system recovers from a step-like disturbance within 7 microseconds. Recorded AFM images verify a significant performance improvement of the model-based controlled system over the analog proportional-integral (PI) controlled AFM.

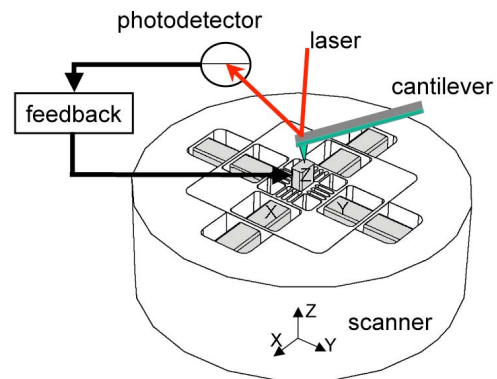


Fig. 1. Scheme of a high-speed AFM.

## I. INTRODUCTION

The continuing development and demand for nanofabrication as well as research in life science require better tools for nanotechnology. The atomic force microscope (AFM)[1] is one of the most important tools to image and manipulate on the nanometer level. For some applications such as imaging biological systems in real-time, however, current commercial AFMs are about two orders of magnitudes too slow, which puts a high demand on ongoing instrument development.

The principle of the AFM (see Figure 1) is that the vertical (Z-direction) force interaction between the sample and a very sharp tip is held constant while either of them is scanned relative to the other. This is done by feedback operation on the static deflection of the cantilever (in contact mode or constant force mode) or on the amplitude of the oscillating cantilever (in dynamic or tapping mode). For an overview see e.g. [2] and references therein.

In all measurement modes AFM operation can be split into two main tasks, namely i) the scanning motion and ii) controlling the tip-sample interaction force, given by the (static or dynamic) deflection of the cantilever.

One of the main issues in AFM instrumentation still is the imaging speed [3]. Commercial AFM systems typically take between several seconds and a few minutes to acquire one image. For direct observation of molecular

processes, however, imaging at video-rates (25 frames per second) would be desirable. Recent advances in AFM-instrumentation demonstrated feasibility of real-time imaging at the nano-meter scale with the AFM [3][4][5]. Improvements in imaging speed have been reported by re-designing the scanning unit [4][6][7] to achieve a faster response, as well as by applying modern control methods. Improved control of the scanning motion has been demonstrated by damping of the actuator's resonances [8] as well as by applying model-based feedforward [9][10] or feedback control [11][12] or iterative learning control [13]. Tracking of the sample topography has been improved by better control of the tip-position using model-based feedback [14], by an internal model control approach [15], by a gain-scheduling approach [16], and by feedforward compensation [17] of the estimated sample-profile.

Although the image acquisition and scanning speed of some prototype AFMs is impressive, the feedback bandwidth for tracking the sample topography with the AFM-tip still has to be improved for imaging soft biological tissue (see [3]). This paper presents an analog implementation of a model-based feedback controller on a field programmable analog array (FPAA), which enables a control bandwidth beyond 100 kHz with tight control demands for high-speed AFM imaging at reduced variations of the imaging force. The implementation of a model-based feedback controller,

\* Corresponding author: Georg Schitter (phone: +31-15-278-6152; email: g.schitter@tudelft.nl)

designed in the  $H_\infty$ -framework, for controlling the vertical (Z) positioning axis of a high-speed AFM demonstrates significant improvements over an analog proportional-integral (PI) feedback controller. The high bandwidth of the control system is demonstrated by recorded AFM images as well as by demonstration of the fast recovery (within  $7 \mu\text{s}$ ) from a step-like disturbance, which emulates the case of the sample topography when scanning at high-speeds.

## II. MODELING OF THE AFM DYNAMICS

The high-speed AFM scanner under investigation is a prototype of a flexure-based scanner (cf. [7]), which is designed for high resonance frequencies in order to achieve a fast response. The piezoelectric stack actuators are driven with custom made amplifiers. Coupling between the individual positioning axis has been minimized during the device design.

For modeling and control, the input to the power amplifier for the vertical positioning axis is regarded as the system input. The system output is given by the deflection of the AFM cantilever sensing the position of the Z-piezo.

### A. Vertical Dynamics

The scanner dynamics in the vertical direction have been characterized by applying a sweep signal to the power amplifier of the Z-piezo. The Z-piezo's position, regarded as the system output, is sensed by an AFM-cantilever (resonance frequency  $> 500 \text{ kHz}$ ) and the AFM's optical deflection detection system. Generation of the input signal and recording of the system's response is done with a network analyzer (HP35639A, Agilent, Palo Alto, CA, USA).

Figure 2 shows the measured frequency response between 10 and  $300 \text{ kHz}$  for excitation amplitudes of 1 mV, 25 mV, and 50 mV at the input of the power amplifier, demonstrating the linearity of the system's dynamics. Potential nonlinearities of the piezo actuator, such as hysteresis and creep, are compensated by the feedback loop and have to be considered at the data acquisition side when recording and displaying the AFM signals.

The frequency response in Z-direction reveals two resonance-anti-resonance pairings due to the integration of the piezo in the scanner structure (cf. [7]) at 70 and 100 kHz, respectively, and three resonances between 150 and 200 kHz, which can be attributed to the Z-piezo itself. A fitted  $10^{\text{th}}$ -order mathematical model of the scanner is shown by the solid black line in Fig. 2.

This model is also chosen as the nominal model of the scanner for the controller design (see Section III-A). Figure 3 demonstrates the good agreement between the simulated step-response of the modeled system (solid black line) and the measured step-response (dotted red line). The weakly damped multiple resonances of this system are obvious by the aggressive initial response and the slow

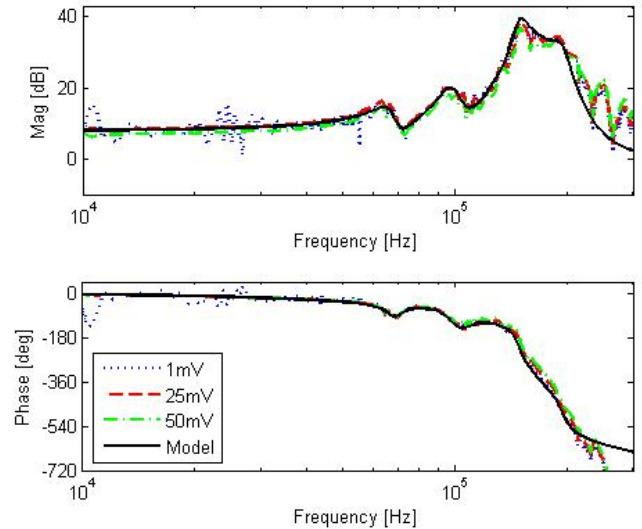


Fig. 2. Frequency response of the AFM in vertical direction, measured at various amplitudes (coloured lines) and simulated response of the fitted model (solid black line).

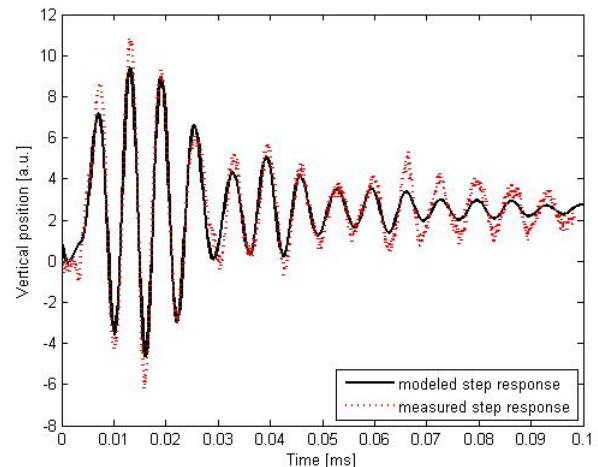


Fig. 3. Step response of the AFM in vertical direction. Measured response (dotted red); simulated response of the  $10^{\text{th}}$  order model (solid black).

decay of the oscillations in the Z-piezo's position.

## III. CONTROLLER DESIGN

The oscillatory behavior of the AFM scanner imposes limitations to the achievable imaging speed. In Z-direction the higher order oscillatory modes (see Figs. 2 and 3) cannot be compensated by a simple PI controller, and therefore limit the achievable closed-loop bandwidth for tracking the sample topography with PI-feedback. For such oscillatory systems a model-based feedback controller, which is derived in the this section, enables to achieve a higher closed-loop bandwidth (cf. [14]).

### A. Controller for Topography Tracking

Figure 4 shows a block-diagram of the AFM topography measurement system. The blocks connected by solid lines form the control-loop for tracking the sample topography. During this feedback operation two signals are recorded, forming the AFM images (i) the topography signal, which is represented by the control action  $u$ , and (ii) the deflection signal, which correspond to the residual control error  $e$ . The control goal is to keep the cantilever deflection close to the deflection setpoint denoting the nominal imaging force, which means to keep variations of the imaging force small and to shift as much information as possible from the deflection image to the topography image (cf. Fig. 11).

The frequency response (Fig. 2) and step response (Fig. 3)

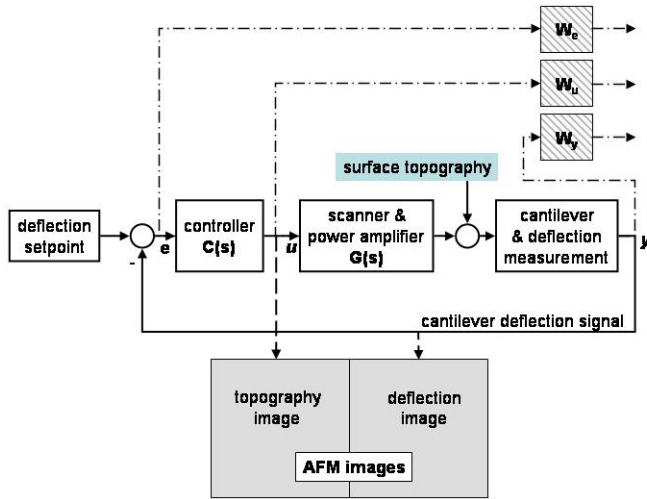


Fig. 4. Schematic of the AFM topography measurement system. The blocks connected by solid lines form the control loop of the AFM in Z-direction. The dashed lines show the signals recorded to display the AFM images. The dash-dotted lines indicate the weighting functions of the extended model for the design of the  $H_\infty$ -controller.

of the scanner in Z-direction shows several slightly damped resonances of this positioner. To achieve a high closed-loop bandwidth in combination with good robustness a model-based feedback controller for the AFM-system in Z-direction is designed. This controller is based on the fitted  $10^{th}$ -order mathematical model presented in Fig. 2. This mathematical model (comprised of the blocks between  $u$  and  $y$  in Fig. 4) is extended by the weighting functions  $W_e$ ,  $W_u$ , and  $W_y$ , as indicated by the dash-dotted lines in Figure 4. The feedback controller  $C(s)$  is designed in the  $H_\infty$ -framework by a mixed sensitivity design [18], as is also described in a similar application in [17].

The weighting function  $W_u$  is set constant. The weighting function  $W_y$  defines the upper bandwidth for the reliability of the model  $G(s)$  and is fine tuned to shape the loop. In the design step the weighting function  $W_e$  is increased in its bandwidth as much as possible in order to achieve fast tracking of the closed-loop controlled system with the requirement of no oscillations in the position of the Z-piezo. Figure 5 shows the singular values of the weighting functions

for the control error ( $W_e$ ) and for the output tracking ( $W_y$ ), as well as the achieved sensitivity  $S$  and complementary sensitivity  $T$  when closing the loop with the  $H_\infty$ -feedback controller, derived using Matlab (The MathWorks, Natick, MA, USA). The resulting controller is

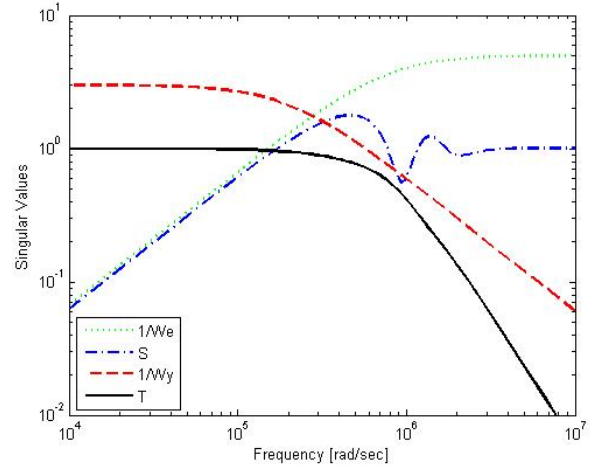


Fig. 5. Weighting function  $1/W_e$  (dotted green) and  $1/W_y$  (dashed red) for the  $H_\infty$  controller design, and achieved sensitivity  $S$  (dash-dotted blue) and complimentary sensitivity  $T$  (solid black).

of  $12^{th}$  order and can be balanced and reduced to  $10^{th}$  order without significant loss of control performance. The simulated response of the closed-loop controlled system to a step-like input signal settles in less than  $10 \mu s$  to within two percent of the steady-state position, as shown in Figure 6. In case case of the  $12^{th}$  order controller the system settles without any oscillations. For the  $10^{th}$  order controller the specifications are still met, and only very small oscillations in the Z-position can be observed (Fig. 6(b)). Since the complexity of the  $12^{th}$ -order controller is close to

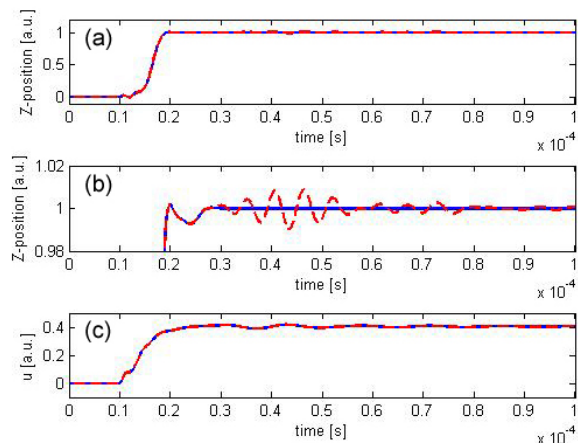


Fig. 6. Simulated step-response of the closed-loop system, controlled with the  $12^{th}$ -order (solid blue lines) and a  $10^{th}$ -order  $H_\infty$ -controller (dashed red lines), respectively. The step in the input signal (not shown) occurs at time  $0.1 \cdot 10^{-4}$  s. (a) controlled position of the Z-actuator; (b) zoom onto the 2-percent-band around the steady-state position of (a); (c) control action  $u$ .

the maximum capability of the used control hardware [19], and the 10<sup>th</sup>-order controller also meets the specified control performance, only the 10<sup>th</sup>-order controller is implemented and tested on the AFM setup.

### B. Controller Implementation on FPAA

For an effective implementation of the new feedback controller the control-hardware has to fulfill the following three requirements:

- For a bandwidth of more than 100 kHz and the tight control objectives (fast settling time without oscillations), the sampling rate of a digital controller should be at least 1 MHz.
- The resolution of the D/A-converter of a digital control system has to be 16-bit or higher to achieve the required accuracy over the entire positioning range of the Z-actuator.
- The controller should be easy to implement and modify for varying applications of the AFM.

The high demand on the fast sampling rate excludes most digital signal processors (DSP) enabling floating point operation from the choice for the implementation of the feedback controller. Field programmable gate arrays (FPGA) may give the high sampling frequency, but due to the fixed point implementation programming is tedious and easy and fast modification is not possible. A new type of hardware (see e.g. [20]) that fulfills all the above listed requirements are field programmable analog arrays (FPAA). These analog arrays are based on switched capacitor filters with a switching frequency up to 16 MHz [19]. The analog nature of these circuits omits the quantization issue completely, and the achievable resolution is determined only by the system's signal-to-noise ratio. Furthermore, programming of these circuits is fast and easy and can be updated on the fly. The used FPAA's development boards [19] allow implementation of first- and second-order elements (bilinear and biquadratic filters) with left half-plane poles and zeros.

$$G(s)_{bilin} = \frac{s + \omega_z}{s + \omega_p}, \quad (1)$$

$$G(s)_{biquad} = \frac{s^2 + 2\zeta_z\omega_zs + \omega_z^2}{s^2 + 2\zeta_p\omega_ps + \omega_p^2}, \quad (2)$$

with frequencies  $f_z = \omega_z/(2\pi)$  and  $f_p = \omega_p/(2\pi)$  and quality-factors  $Q_z = 1/(2\zeta_z)$  and  $Q_p = 1/(2\zeta_p)$  of poles and zeros, respectively. It should be noted that these FPAA's cannot implement non-minimum phase zeros, which may be accounted for in the design and implementation of the controller.

For the implementation, the above designed 10<sup>th</sup>-order controller has to be converted into a biquadratic structure. This is done by transforming the state space representation of the controller into a zero-pole-gain representation, using the Matlab command *zpk*, and by combining (pairs of) poles and zeros with neighboring frequencies to first- and second order subsystems. These first and second order subsystems, given by their transfer functions (1) and (2), can

directly be implemented in the FPAA software using pre-defined elements, where the user adjusted parameters are the respective frequency and damping of the corresponding poles and zeros. The higher-order controller  $C(s)$  eventually is realized by connecting the first and second order filters in series

$$C(s) = \frac{K_I}{s} \prod_i G(s)_{bilin(i)} \prod_j G(s)_{biquad(j)}, \quad (3)$$

where the factor  $K_I$  corresponds to an integral gain and  $i$  and  $j$  are the respective indices of the bilinear (1) and biquadratic filters (2). The FPAA is eventually programmed via a serial connection with the development-board.

Figure 7 shows the user interface for programming the FPAA, showing the structure of the 10<sup>th</sup>-order feedback controller implemented at a switching frequency of 4 MHz. The first element of the implemented controller is a summing stage for calculating the error signal. The second element is an integrator, followed by four biquadratic and one bilinear filter.

In order to scale and interface the differential input of

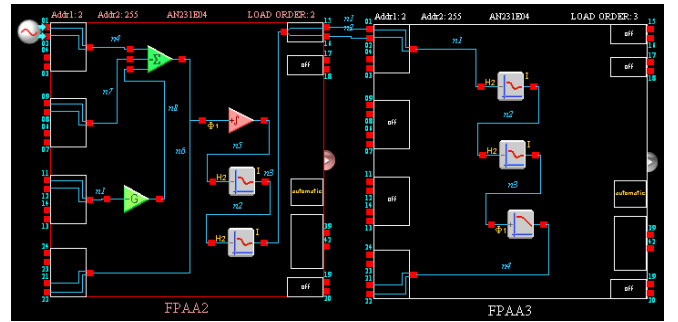


Fig. 7. User interface for the implementation of the 10<sup>th</sup> order filter on the FPAA. Reprogramming the FPAA on the fly via a serial connection allows for fast and easy changes of the implemented feedback controller.

the FPAA with the single-ended AFM signals, we used operational amplifiers AD-8132 (Analog Devices, Norwood, MA, USA). The differential FPAA-output signal has been scaled and converted to a single-ended signal using an operational amplifier AD-8130 (Analog Devices), and consecutively has been connected to the power amplifier driving the Z-piezo.

In order to characterize the achieved closed-loop performance we measured the sensitivity function  $S$  and complementary sensitivity  $T$ , as is shown in Figure 8. The sweep-signals for measuring  $S$  and  $T$  are generated with the network analyzer and are applied to the closed-loop system by using an additional input of the FPAA, which is connected with the summing stage for the error signal generation (see Fig. 7). The corresponding response signal for  $S$  and  $T$  is recorded by the network analyzer via an additional output of the FPAA. Tuning of the integral gain of the FPAA has been done during AFM imaging (see Figs. 10 and 11) in order to increase the imaging bandwidth as much as possible, which explains the slightly higher bandwidth

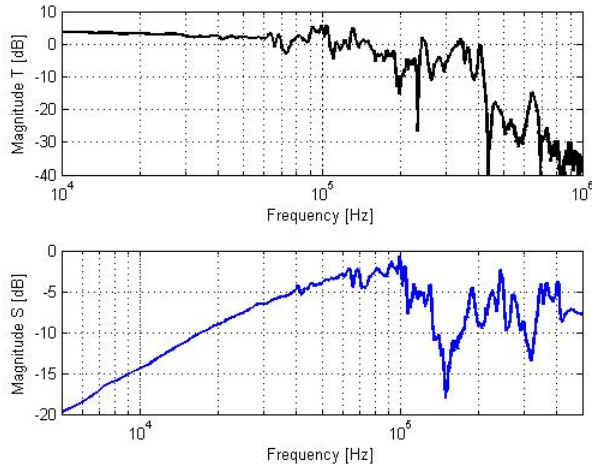


Fig. 8. Measured complementary sensitivity function  $T$  and sensitivity function  $S$  of the feedback loop in  $Z$ -direction.

of the measured curves of  $S$  and  $T$  as compared to the simulation. One can observe some additional small peaks in the measured spectra of  $S$  and  $T$  (Fig. 8) as compared to the simulated responses (cf. Fig. 5), which may result from noise at the FPAA-output and from un-modeled higher modes of the AFM positioning system, but in general the measurement reflects the predicted behavior very well.

To further characterize the closed-loop response a step-like

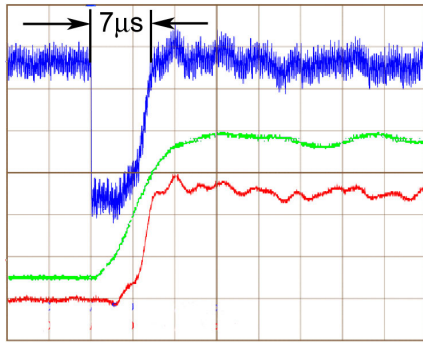


Fig. 9. The  $H_\infty$ -controlled closed-loop system recovers from a step-like disturbance within  $7 \mu s$ . Control error signal (blue,  $0.1 \text{ V/div}$ ) recorded at an auxiliary FPAA output; Control action (green,  $2 \text{ V/div}$ ) recorded at the output of the  $Z$ -piezo's power amplifier; Cantilever deflection signal (red,  $0.5 \text{ V/div}$ ) at the AFM output; time-scale:  $5 \mu s/div$ .

disturbance signal has been applied to the AFM control loop. This signal is added to the cantilever deflection, which has the same effect to the closed-loop for tracking the sample topography as a topographical step in the sample surface. Figure 9, recorded with a digital oscilloscope, shows that the closed-loop system fully recovers from the step-like disturbance within  $7 \mu s$ , displaying the control error  $e$  measured at an additional FPAA output (blue line), the control action  $u$  measured at the output of the power amplifier of the  $Z$ -piezo (green line), and the cantilever deflection measured at the AFM system

(red line). Please note that the error signal returns to its initial value (zero), whereas the cantilever deflection does not since the disturbance step has been added to it after the point where the deflection is recorded. The apparent high noise-level on the FPAA output (blue signal) are high-frequency oscillations due to the switching-frequency of the capacitors, which get suppressed by the low-pass characteristics of the power amplifier driving the  $Z$ -piezo (green signal).

#### IV. IMAGING RESULTS

For imaging applications with the high-speed AFM lateral oscillations of the scanner are suppressed by model-based filtering of the scanning signal in order to avoid imaging artifacts due to turn-around ripples (see [10]).

To demonstrate the benefit of the new feedback controller we imaged a silicon calibration grating as a test sample. Figure 10 shows deflection images recorded in contact mode at a speed of 95 lines per second, recorded with the PI-feedback and the  $H_\infty$ -feedback controlled AFM, respectively. To demonstrate the repeatability of the system response the slow scan axis has been disabled, resulting in re-imaging the same scan-line over and over again and stacking the consecutive responses of the same line together to one image. In case

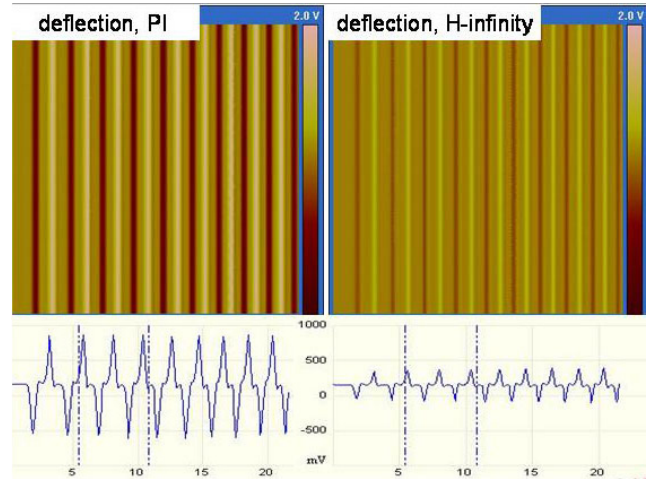


Fig. 10. Comparison of the residual control error of the PI-controlled AFM (left image) and the  $H_\infty$ -controlled one (right image). The lower panels show cross sections of single scan lines from the images above them, demonstrating the reduction of the cantilever deflection by a factor of 3. The imaged sample is a silicon calibration grating with  $100 \text{ nm}$  deep squared holes at a pitch of  $1 \mu m$  scanned at a speed of 95 lines per second.

of the  $H_\infty$ -controller the cantilever deflection (denoting the residual control error) is reduced by a factor of about 3, as is obvious when comparing the cross sections given in the lower two panels of Fig. 10. This significant reduction of the cantilever deflection results in lower variations of the average imaging force and also enables further reduction of the minimum force point without loss of tip-sample contact.

Figure 11 shows the topography (left) and deflection (right)

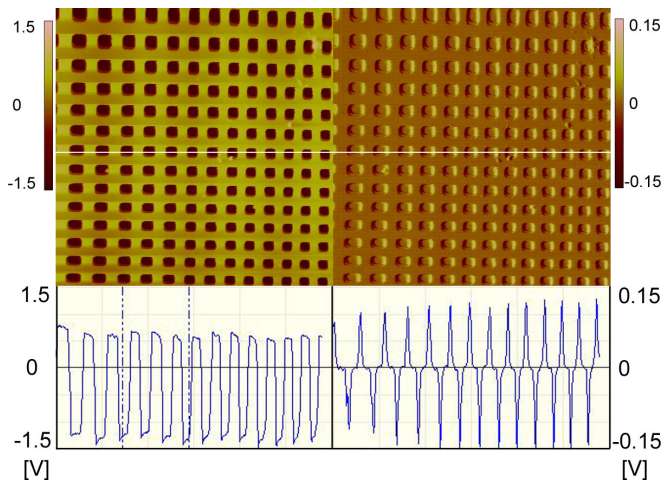


Fig. 11. Topography (left) and deflection (right) images of a silicon calibration grating with a pitch of  $1 \mu\text{m}$ , recorded with the  $H_\infty$ -controlled AFM at 47 lines per second. The lower panels show cross sections marked by the white line in the images.

image of a calibration grating, recorded with the  $H_\infty$ -controlled system at a scan-speed of 47 lines per second and a resolution of 512 by 512 pixels. The fast scanning direction is aligned with the horizontal axis of the images, the recording direction is from left to right. The high feedback bandwidth is obvious by the small ( $<150 \text{ mV}$ ) deviations from the nominal cantilever deflection of 0 V. In this imaging example the feedback-system has to handle over 2400 step responses per second, and still manages a fast return to the nominal cantilever deflection, given by the dominant brown color in the deflection image.

## V. CONCLUSION

This contribution presents the successful implementation of a new feedback controller for a high-speed AFM. Field programmable analog arrays enables an easy, fast, and re-programmable implementation of higher-order feedback controllers for control applications at high bandwidths. A model of the AFM dynamics in the vertical positioning direction is derived, and a model-based feedback controller for tracking the sample topography at a control bandwidth on the order of 100 kHz is designed in the  $H_\infty$ -framework. A measured step response demonstrates that the closed-loop system fully recovers from a step like disturbance within  $7 \mu\text{s}$ . The successful implementation of the  $10^{\text{th}}$ -order  $H_\infty$  feedback controller on the FPAA demonstrates a significant improvement over the PI-controlled AFM system. The fast imaging capabilities and high feedback bandwidth of the prototype AFM are demonstrated by imaging a test specimen at high speed. The significant reduction in the residual cantilever deflection by means of the new feedback system is an important step towards gentle imaging of fragile biological specimens in real-time.

## VI. ACKNOWLEDGMENTS

The authors would like to thank Prof. Tsu-Chin Tsao from UCLA for fruitful discussions.

This work is supported in part by TU-Delft 3mE faculty grant PAL-614, by the Netherlands Organization for Scientific Research (NWO) under Innovational Research Incentives Scheme (VENI DOV.7835), and by the National Institutes of Health under Award RO1 GM 065354-05.

## REFERENCES

- [1] G. K. Binnig, C. F. Quate, and C. Gerber, "Atomic force microscope," *Phys. Rev. Lett.*, vol. 56(9), pp. 930–933, 1986.
- [2] D. Abramovitch, S. Andersson, L. Pao, and G. Schitter, "A tutorial on the mechanisms, dynamics, and control of atomic force microscopes," in *Proceedings of the 2007 American Control Conference, AACC*. New York, NY: IEEE, July 11–13 2007, pp. 3488–3502.
- [3] P. Hansma, G. Schitter, G. Fantner, and C. Prater, "High speed atomic force microscopy," *Science*, vol. 314, pp. 601–602, 2006.
- [4] T. Ando, T. Kodera, E. Takai, D. Maruyama, K. Saito, and A. Toda, "A high-speed atomic force microscope for studying biological macromolecules," *Proc. Nat. Acad. Sci.*, vol. 98, pp. 12 468–12 472, 2001.
- [5] A. Humphris, M. Miles, and J. Hobbs, "A mechanical microscope: High-speed atomic force microscopy," *Appl. Phys. Lett.*, vol. 86(3), p. 034106, 2005.
- [6] J. Kindt, G. Fantner, J. Cutroni, and P. Hansma, "Rigid design of fast scanning probe microscopes using finite element analysis," *Ultramicroscopy*, vol. 100(3-4), pp. 259–265, 2004.
- [7] G. Schitter, K. Åström, B. DeMartini, P. Thurner, K. Turner, and P. Hansma, "Design and modeling of a high-speed afm-scanner," *IEEE Trans. Contr. Syst. Technol.*, vol. 15(5), pp. 906–915, 2007.
- [8] A. Fleming and S. Moheimani, "Sensorless vibration suppression and scan compensation for piezoelectric tube nanopositioners," *IEEE Trans. Contr. Syst. Technol.*, vol. 14(1), pp. 33–44, 2006.
- [9] D. Croft, G. Shed, and S. Devasia, "Creep, hysteresis, and vibration compensation for piezoactuators: Atomic force microscopy application," *ASME J. Dyn. Syst. Meas. Contr.*, vol. 128(35), pp. 35–43, 2001.
- [10] G. Schitter and A. Stemmer, "Identification and open-loop tracking control of a piezoelectric tube scanner for high-speed scanning-probe microscopy," *IEEE Trans. Contr. Syst. Technol.*, vol. 12(3), pp. 449–454, 2004.
- [11] S. Salapaka, A. Sebastian, J. P. Cleveland, and M. V. Salapaka, "High bandwidth nano-positioner: A robust control approach," *Review of Scientific Instruments*, vol. 73, no. 9, pp. 3232–3241, 2002.
- [12] A. Sebastian and S. Salapaka, "Design methodologies for robust nano-positioning," *IEEE Trans. Contr. Syst. Technol.*, vol. 13(6), pp. 868–876, 2005.
- [13] K. Leang and S. Devasia, "Design of hysteresis-compensating iterative learning control for piezo-positioners: Application to atomic force microscopes," *Mechatronics*, vol. 16, pp. 141–158, 2006.
- [14] G. Schitter, P. Menold, H. Knapp, F. Allgöwer, and A. Stemmer, "High performance feedback for fast scanning atomic force microscopes," *Rev. Sci. Instrum.*, vol. 72, no. 8, pp. 3320–3327, 2001.
- [15] N. Kodera, H. Yamashita, and T. Ando, "Active damping of the scanner for high-speed atomic force microscopy," *Rev. Sci. Instrum.*, vol. 76, p. 053708, 2005.
- [16] N. Kodera, M. Sakashita, and T. Ando, "Dynamic proportional-integral-differential controller for high-speed atomic force microscopy," *Rev. Sci. Instrum.*, vol. 77, pp. 083 704–1–083 704–7, 2006.
- [17] G. Schitter, A. Stemmer, and F. Allgöwer, "Robust two-degree-of-freedom control of an atomic force microscope," *Asian Journal of Control*, vol. 6(2), pp. 156–163, 2004.
- [18] S. Skogestad and I. Postlethwaite, *Multivariable Feedback Control*. Wiley, 1996.
- [19] *Field Programmable Analog Array: AN231K04-DVLP3 - AnadigmApex Development Board*, Anadigm Inc., Campbell, CA, USA, 2006.
- [20] L. Znamirovski, O. Palusinski, and S. Vrudhula, "Programmable analog/digital arrays in control and simulation," *Analog Integrated Circuits and Signal Processing*, vol. 39, pp. 55–73, 2004.